RSC Advances

ROYAL SOCIETY OF CHEMISTRY

www.rsc.org/advances

Multicolor Luminescent Hybrid Assembled Materials Based on Lanthanide-Containing Polyoxometalates Free From Energy Transfer Crosstalk

Nan Shi, Yan Guan, Jie Zhang*, Xinhua Wan*

Beijing National Laboratory for Molecular Sciences, Key Laboratory of Polymer Chemistry and Physics of Ministry of Education, College of Chemistry and Molecular Engineering, Peking University, Beijing 100871, China

Abstract

A series of multicolor luminescent hybrid materials based on three primary molecular pixel components, isostructural lanthanide-containing inorganic clusters LnW_{10}, i.e. red-emissive $Na_9EuW_{10}O_{36}$ (EuW_{10}) and green-emissive $Na_9TbW_{10}O_{36}$ (TbW_{10}), and a blue-emissive small organic molecule quinine were constructed in a general and straightforward way. The neutral-cationic block copolymer poly(ethylene oxide)$_{114}$-*b*-poly(2-(2-guanidinoethoxy)ethyl methacrylate)$_{23}$ (PEO_{114}-*b*-PGu_{23}) electrostatically co-assembles with the inorganic clusters LnW_{10} into micelles, and consequently effectively prohibits the energy transfer between LnW_{10} and quinine. Three luminescent elements possessing their independent emission properties in supramolecular assemblies, like molecular pixels, were deeply investigated for the first time. On the basis of additive color theory, fluent emitting color changes within the triangle enclosed by the luminophores in chromatic diagram were achieved at diverse mixing ratios and exciting wavelengths with precise prediction and convenient reproduction.

Introduction

Multicolor luminescent materials have attracted extensive considerations in the past few decades for their potential applications in realms of full-color displays[1-4] and luminescence probes[5-8]. According to additive color theory, three primary colors red, green, and blue, or two compensate colors such as yellow and blue are traditionally required to generate a full-color, particularly white-color, luminescence[9-12]. Up to now, a considerable amount of multicolor-emitting materials have been reported, including small organic molecules[13-15], metal compounds[16], conjugated polymers[17, 18], metal-doped hybrid materials[19-21], polymeric nanomaterials[22-25], and supramolucular materials[26-29].

However, unwanted energy transfer between luminophores is almost inevitable due to the highly populations of excited states of donors and ground states of acceptors under illumination[30]. As a result, through tedious and laborious repetitions of tuning mixing ratios and altering excitation wavelengths, a desired emission color can be obtained. Besides, energy transfer efficiency is extremely enhanced with the increased luminophores concentrations and the decreased distances[31], resulting in overwhelmingly dominant emission from lower bandgap components rather than the relatively higher bandgap ones. Moreover, as the extent of energy transfer is closely correlated to fabrication process of devices, reproduction of emission color is another challenge even in a certain situation. Up till now, more and more researches have been reported upon effective avoidance of energy transfer crosstalk. Park's group[32] created a molecular pixel system composed of delicately designed excited-state intramolecular proton transfer RGB-emitting dyes, which not only blocks undesired energy transfer, but also precisely predicts and reproduces the whole gamut in CIE 1931 diagram enclosed by the dyes in both solutions and films. Besides, with the help of site isolation mechanism, Fréchet's group[33] built up cross-linked luminescent polymer nanoparticles to minimize energy transfer between chromophores. Hitherto, even though tremendous efforts have been dedicated to developing multicolor materials free from energy transfer, constructing a totally frustrated energy transfer system in a simple and general approach including both molecular synthesis and material fabrication is still challenging.

Among all the luminophores, lanthanide-containing molecules[34-37] (lanthanide complex, LnMOF, lanthanide-polyoxometalates, and so on) are promising candidates for designing multi-color luminescent materials because of their diverse colorful emissions, high photoluminescent efficiencies, large Stocks' shifts, and narrow emission band[38-40]. However, these rigid inorganic luminophores are not appropriate for further fabrications. Two strategies were commonly applied to improve their processability[41]. One is by co-doping red (Eu^{3+} and Sm^{3+}) and green (Tb^{3+} and Er^{3+}) emitting Ln^{3+} ions with a certain blue-light emission source into varied matrix, but microphase separation usually occurs[42]; the other one is to dope multiple isostructural analogous of lanthanide complexes to precisely control the output emissions[43, 44]. Nevertheless, the universal existence of energy transfer between lanthanide ions[45] or antenna effect between the lanthanide and emitting organic ligands[46, 47] restricts their potential applications as molecular pixels. Furthermore, time-consuming one-to-one chemical synthesis is also frequently involved in the two approaches above, *i.e.*, once the

luminescent requirements altered, synthesis has to be proceeded to prepare desirable materials. Herein, to minimize the undesired energy transfer and simplify the synthesis, we created a molecular pixel system in a general way based on inorganic-organic hybrid supramolecular assemblies composed of natural-cationic double hydrophilic block copolymer (BCP) and luminescent molecules. Lanthanide-polyoxometalates, $Na_9EuW_{10}O_{36}$ (EuW_{10}) and $Na_9TbW_{10}O_{36}$ (TbW_{10}), were introduced as red- and green-color emitting molecules, respectively, and organic quinine as the blue light source. In this work, LnW_{10} (Ln = Eu, Tb) were incorporated into the core of micelles by cocervate complexation with the cationic block of PEO_{114}-*b*-PGu_{23}, while quinine molecules are dispersed outside the micelles in both solvent and matrix, spatially isolated with LnW_{10}. The BCPs surround each LnW_{10} and the electrostatic repulsion between inorganic clusters separated LnW_{10} in space. The spatial isolation between those chromophores/luminophores effectively blocked undesired energy transfer, offering these luminophores an opportunity to act as a set of molecular pixels. The three primary color emitting molecules created a triangle named gamut in CIE 1931 chromaticity diagram where fluent color changes within the triangle can be precisely predicted and conveniently reproduced at various mixing ratios and excitation wavelengths.

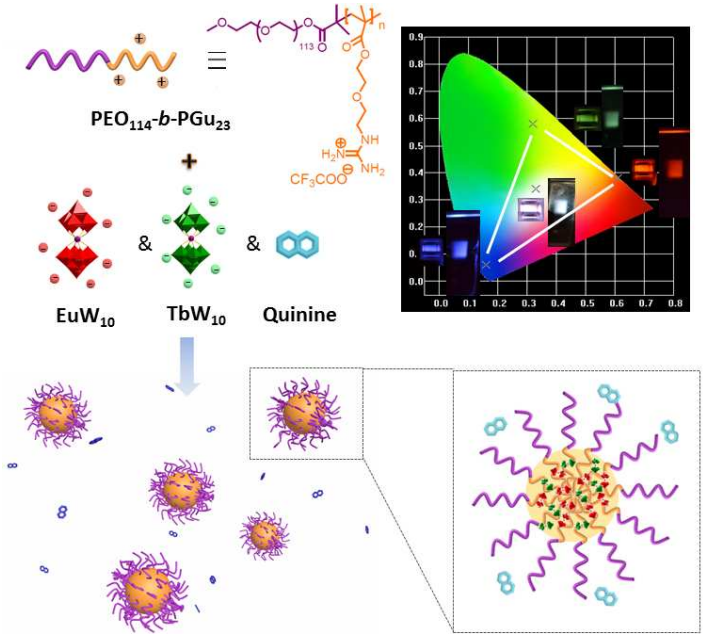

Scheme 1 Schematic illustration of the luminescent hybrid assembly and the CIE 1931 chromaticity diagram. The insets are photographs of primary color and white color mixture solutions and films illuminated at 280 nm ultraviolet source.

Experimental section

Materials

2-Bromo-2-methylpropionyl bromide, Quinine, *N,N'*-bis(tert-butoxycarbonyl)-1*H*-pyrazole-1-carboxamidine, 2-(2-aminorthoxy) ethanol and *N,N,N',N'',N''*-Pentamethyldiethylenetriamine (PMDETA) were purchased from Tokyo Chemical Industry Co. and used as received. Methoxy poly (ethylene glycol) (CH_3O-PEO_{114}-OH, average M_n ~ 5,000 g/mol) was obtained from Aldrich without further purification. Methacryloyl chloride was purchased from J&K Chemical and distilled just prior to use. Copper (I) bromide (CuBr) was stirred in glacial acetic acid for at least 5 h, then filtered, washed with acetic acid, ethanol, acetone, and ethyl ether, successively, and dried under vacuum before use. Tetrahydrofuran (THF) was distilled over sodium/benzophenone under N_2 protection. Dichloromethane (CH_2Cl_2) and triethylamine (TEA) were dried over CaH_2 and distilled. All aqueous solutions were prepared using ultrapure water from a Millipore Milli-Q system. Unless otherwise noted, the other chemicals were purchased from Sinopharm Chemical Reagent Co. Ltd and used without further purification. Quartz substrates were washed with H_2SO_4 and deionized water, and dried under N_2 atmosphere.

Preparations

EuW_{10} and TbW_{10} were synthesized according to literature reports[48]. The preparation of monomer 2-[2-(*N,N'*-di-*tert*-butoxycarbonylguanidino)ethoxy] ethyl methacrylate (BocGEEMA) was reported in our previous work[49], and the block copolymer PEO_{114}-*b*-PGu_{23} was prepared through atom transfer radical polymerization (ATRP), initiated by macroinitiator PEO_{114}-Br, as illustrated in Fig.1. Detailed synthetic procedures were described in Supporting Information.

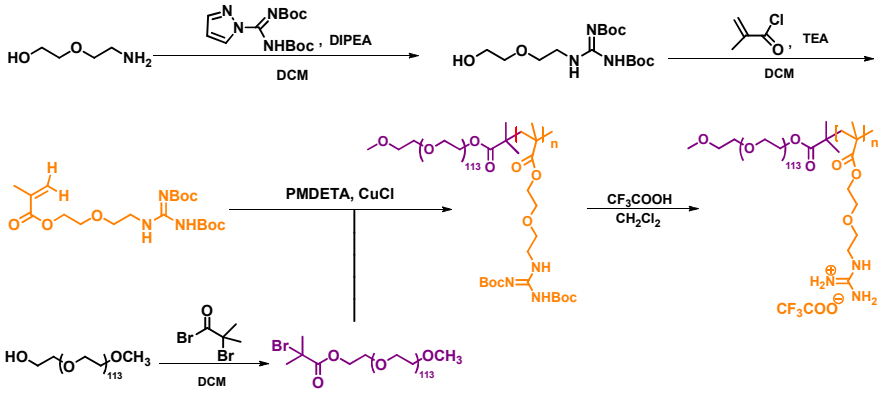

Fig.1 Synthesis process of neutral-cationic block copolymer.

All aqueous mixture solutions in this work were prepared as follows: aqueous solutions of individual components required (*e.g.* TbW_{10} solution, and/or EuW_{10} solution, and/or quinine solution, and/or PEO_{114}-*b*-PGu_{23}) were mixed under vigorous stirring in stoichiometric ratios, followed by standing overnight. The total concentration of LnW_{10} in each LnW_{10}-containing mixture is 3.50×10^{-5} M and that of the copolymer is 1.37×10^{-5} M for spectroscopic measurements. For the quinine/copolymer solution, the concentration of quinine is controlled 3.50×10^{-5} M.

To fabricate the photoluminescent films, poly(methyl methacrylate) (PMMA) (Mw = 120000 g/mol) was introduced as the matrix. The as-prepared aqueous solutions were extracted with a chloroform solution of PMMA under vigorously stirring over 48h, then the organic phase was collected, casted on a quartz plate, and dried in air.

Measurements

The molecular weight and molecular weight distribution were determined by a gel permeation chromatography (GPC) apparatus equipped with a Waters 2410 refractive-index detector and a Waters 515 pump. ^{1}H NMR spectra were recorded on a Bruker AVANCE Ⅲ spectrometer (400 MHz). ICP data were obtained on Profile Spec (Leeman). An FLS920 Steady State & Time-resolved Fluorescence Spectrometer (Edinburgh Instruments Ltd.) was used to measure the photoluminescence intensity and life time of the emission from solutions and films. The luminescence decays were fitted via the following equation:

$$I(t) = \sum a_i \exp\left(-t / \tau_i\right)$$

where a_i represents fractional contribution to the total luminescence decay. Photoluminescence quantum yields (PLQY) were measured by absolute PL quantum yield measurement system C9920-02 upon excitation at 280 nm. Dynamic light scatter (DLS) measurements were performed on a commercialized spectrometer from Brookhaven Instrument Corporation (BI-200SM Goniometer, Holtsville, NY). A vertically polarized, 100 mW solid-state laser (GXC-III, CNI, Changchun, China) operating at 633 nm was used as the light source, and a BI-TurboCo digital correlator (Brookhaven Instruments Corp.) was used to collect and process data. The samples were filtered through 450nm filters and the scattering angle was 90°. TEM images were obtained on a JEM-2100 (JEOL, Japan) transmission electron microscopy operated at 200 KV. The samples were prepared by dipping a drop of solution onto copper grids coated with amorphous carbon membranes and then drying in air.

The expected emission spectra were achieved by simply superimposing the measured emission spectra of primary solutions excited at corresponding wavelengths weighted to their concentrations. From the expected emission spectra, the calculated CIE values were obtained.

Results and Discussion

Assembling behavior of LnW_{10}/ PEO_{114}-*b*-PGu_{23}

Representative transmission electron microscopy images of EuW_{10} (R1), TbW_{10} (G1), TbW_{10}/EuW_{10} = 50/1 (Y1), TbW_{10}/quinine = 10/1 (C1), EuW_{10}/quinine = 5/1 (M1), and TbW_{10}/EuW_{10}/quinine = 50/1/5 (White1) hybrid supramolecular solutions were shown in Fig.2. Well-separated micelles with an average diameter of ~20 nm were observed in every solution containing LnW_{10} and PEO_{114}-*b*-PGu_{23} (PDI = 1.14, show in Fig.S1). As convinced by DLS results, aggregates for samples containing LnW_{10} displayed comparable average hydrodynamic radii, R_h, about 10nm, in good agreement with TEM results. It is known that anionic POMs can associate with cationic polyelectrolytes, and above results show that the PGu blocks electrostatically interact with anionic LnW_{10} to form complex coacervate core micelles (C3Ms) [50, 51].The types of inorganic clusters had no influence on the morphologies and dimensions of the assemblies, which might be attributed that EuW_{10} and TbW_{10} have a similar structure with the same size and charge density.

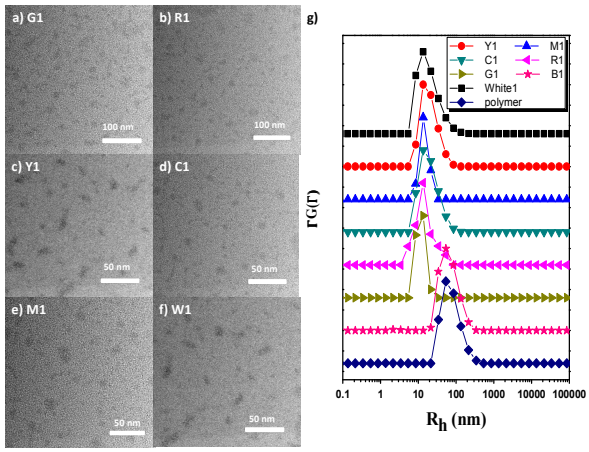

Fig.2 Representative TEM images of a) G1, b) R1, c) Y1, d) C1, e) M1, and f) White1 hybrid assemblies. g) DLS data of the corresponding TEM samples，B1，and BCP solution. The concentrations of the solutions are identical to those of their individual solutions for spectroscopic measurements.

The DLS and TEM results in Fig.2 also indicate that the presence of quinine neither affects morphologies of the original LnW_{10}/block copolymer assemblies nor self-assembled into new aggregates. To further investigate whether quinine molecules go into the micelles or not, the White1 solution was centrifuged, followed by monitoring the luminescent intensities of quinine at the excitation wavelength of 333 nm. The emission intensity of quinine in supernatant was slightly lower than that of the original solution before centrifugation, but almost no quinine was detected in the precipitated micelles (Fig.S2), suggesting that quinine molecules are dispersed in solution rather than being incorporated in micelles.

Based on above results, we proposed a tentative mechanism of the assembly: the cationic PGu blocks and the anionic LnW_{10} electrostatically co-assemble into the interior core of micelles; the hydrophilic PEO blocks constitute the exterior shell and stabilize the micelles in aqueous. Because of its weak interactions with either the block copolymer or LnW_{10}, small molecular quinine are dispersed in solutions

Luminescent properties of primary color-emitting in solutions

The excitation of LnW_{10} (Ln = Eu, Tb) at 280 nm, originated from O→W charge transfer (LMCT), triggered typical Eu^{3+} emissions from $^5D_0$ metastable state to various ^7F_j (j =0, 1, 2, 3, 4) terminal levels[52] and Tb^{3+} emissions from $^5D_0 \rightarrow {}^7F_j$ (j =3, 4, 5, 6) transitions[53], respectively. Quinine emits a broad blue light when excited at 280 nm. After addition of PEO_{114}-*b*-PGu_{23}, LnW_{10} in R1 and G1 displays a greatly enhanced emission (Fig.S4 and Fig.S6), mainly due to replacement of water ligands bound to Ln^{3+} by the copolymer[54]. The emission intensity of quinine slightly decreased after mixing with PEO_{114}-*b*-PGu_{23} (Fig. S8). As for the luminescence decays, two longer lifetimes of 4.01 ms (94.82%) and 1.02 ms (5.18%) were fitted for EuW_{10} in R1 (Fig.S5) than the lifetime of 0.23 ms for EuW_{10} in aqueous solution with the monitoring wavelength of 587 nm. The major one was attributed to EuW_{10} localized in the relatively hydrophobic cores of the micelles while the minor one originated from the single EuW_{10} species in relatively hydrophilic environment[55]. TbW_{10} in G1 monitored at 587 nm has a long lifetime of 2.54 ms (73.70%) assigned to TbW_{10} species in micelles and a short one of 1.16 ms (25.35%) ascribed to single TbW_{10} molecules (Fig.S7). These are similar to the lifetimes monitored at its maximum emission wavelength 542 nm, with a long lifetime ~2.99 ms (77.55%) and a short one ~1.23 ms (22.45%); while a single lifetime of 0.55 ms was observed in

TbW_{10} aqueous solution (Fig. S7). To measure the lifetimes of LnW_{10} at the same time, we chose 587 nm as the monitoring wavelength. The two lifetimes of quinine, 7 ns (~48%) and 3 ns (~52%) does not significantly change in presence of BCP (Fig.S9).

Moreover, the emission spectra of the three molecules covered the whole visible region and their relative intensities can be altered by the excitation wavelengths without obvious variations of shapes (Fig. S10 - Fig. S12), suggesting that fluent emission color changes, as well as white-color emitting, can be achieved by adjusting either mixing ratios or excitation wavelengths. In addition, no effective overlap was observed between the emission spectra in visible areas and the absorption spectra of the red-, green-, and blue-emitting solutions (Fig.S3), indicating that full-color fluorescent system free from energy transfer crosstalk can be established through simple supramolecular assembling.

The assessment of molecular pixels behavior at a fixed wavelength

The suppressed energy transfer assumed from the spectroscopic measurements of EuW_{10}-, TbW_{10}-, and quinine-primary solutions can be evaluated through their binary and ternary mixtures. To settle a set of luminophores competent as molecular pixels, the emission spectra of all the luminophores should be unaffected by each other at a wide range of ratios. Mixtures of either two of the three luminophores at various fractions were prepared to identify independence of their emission spectra. As shown in Fig.3 and Fig.S13- S15, every characteristic band of the individual component can be detected in its corresponding binary mixtures. The solution with a molar ratio of TbW_{10}/EuW_{10}/quinine = 50/1/5 was selected as the representative of ternary mixture solution. Its emission spectrum not only reflects respective transitions of each component, but also covers the full visible region. Significantly, the intensity and shape of the measured spectra can be estimated by straightforwardly superposing the emission spectrum of each component weighted to its molar ratio, further demonstrating block of energy transfer between luminophores. The independence of the emission spectra makes the three luminophores potentially useful as a set of molecular pixels.

The lifetimes of all the mixtures were summarized in Table 1 as another evidence for frustrated energy transfer crosstalk. All the TbW_{10} – EuW_{10} serial solutions took on double-exponential luminescent intensity decays. The long-lived lifetimes ($\tau_2 \approx 3.975$ ms ~ 4.389 ms), comparable to the 4.01 ms of EuW_{10} in R1, with dominant fractions ranging from 92.44% to 74.38% could be assigned to the EuW_{10} species in hydrophobic environments. Both the TbW_{10} and EuW_{10} species contributed

to the short-lived lifetimes ($\tau_1 \approx 1.280$ ms ~ 1.510 ms, 7.56% ~ 25.62%), because the one ~1 ms matched the short lifetime of EuW_{10} species in values and the fractions increased with the increment of TbW_{10} portions. For the LnW_{10} - quinine series, the values and fractions of the lifetimes of Ln^{3+} (Ln=Tb or Eu) were similar to their primary solutions, regardless of the luminophore ratios, inferring that the energy dissipation paths of each lanthanide molecule were unaffected by other luminophores. As we anticipated, the lifetime results of the ternary mixture solution also reflected the identical energy transfer pathways corresponding to individual components.

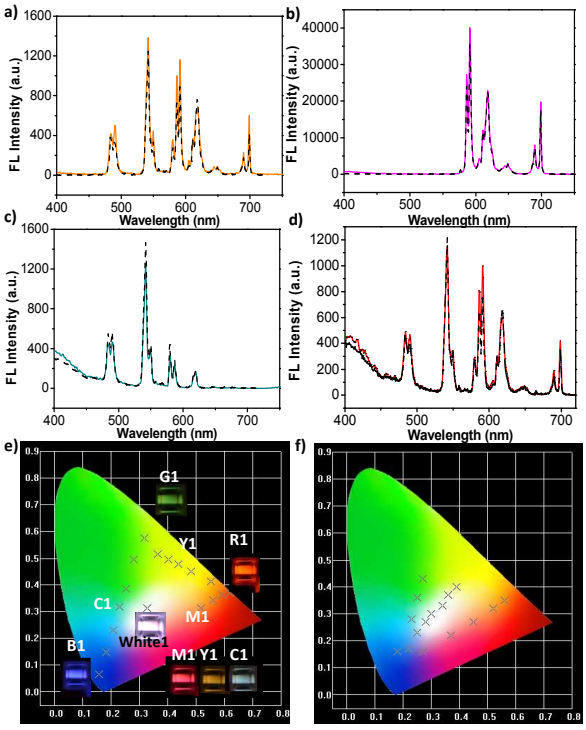

Fig. 3 Emission spectra of a) Y1, b) M1, c) C1, and d) White1. The excitation wavelength is 280 nm. Solid lines indicate the measured spectra and black dashed lines represent expected ones. e) The emission color coordinates of TbW_{10} - EuW_{10}, EuW_{10} - quinine, TbW_{10} - quinine series at different molar ratios, and White1 in the chromaticity diagram. Insets are photographs of representative solution mixtures illuminated under 280 nm. f) The emission color coordinates of TbW_{10}/quinine = 30/1, EuW_{10}/quinine = 3/1, and TbW_{10}/EuW_{10}/quinine = 50/1/3 solutions under different excitation wavelengths in the CIE 1931 chromaticity diagram.

To further evaluate the molecular pixels behavior of these solutions, the emission color coordinates (*x, y*) of all mixtures excited at 280 nm in the CIE 1931 chromaticity diagram were shown in Fig.3

and summarized in Table 1. The chromaticity coordinates were (0.61, 0.38) for EuW_{10}, (0.32, 0.58) for TbW_{10}, and (0.16, 0.06) for quinine-primary solutions, located in the red-, green-, and blue-color region, respectively, and enclosed a triangle gamut that can be generated from additive combinations of the three emissions at its corners. In other words, any chromaticity coordinate on the edge of the triangle can be produced by simple blending proper portions of two of the three corner-emission molecules, and coordinates inside the triangle can be obtained by mixing all the three corner-emission molecules at appropriate ratios. As expected, the EuW_{10} – TbW_{10} series exhibited a continuous color change ranging from red (R1) to yellow (Y1) and finally to green (G1) along the triangle side, and TbW_{10} – quinine series go along the green (G1) - cyan (C1) - blue (B1) edge. The EuW_{10} – quinine has a tendency to go along with the red (R1) - blue (B1) side, but the low solubility of quinine confined the chromaticity coordinates within the red - magenta (M1) range. Fortunately, this problem was resolved by changing the excited wavelength to 310 nm, resulting in a completed red – blue side (Fig.S17), and finally a closed triangle. Patently, the solution composed of EuW_{10}/TbW_{10}/quinine = 50/1/5 created a nearly white emission to the naked-eye with CIE coordinates of (0.34, 0.33). The coordinates also fall well within the white region of the 1931 CIE diagram (for pure white x = 0.33, y = 0.33). Additionally, the measured CIE coordinates are in good agreement with the values calculated from the estimated emission spectra of the corresponding solutions. On this occasion, by simply measuring the emission spectra of the luminophores located at the corners, any target color within the gamut can be estimated and prepared from additive combinations of the three emissions, without the tedious trials.

Luminescent properties upon varying excitation wavelengths

We chose TbW_{10}/quinine = 30/1, EuW_{10}/quinine = 3/1, as well as TbW_{10}/EuW_{10}/quinine = 50/1/3 as examples to investigate the “molecular pixels” behavior excited at distinct wavelengths. The shapes and peaks of the emission spectra in all samples exhibit no obvious deviations in the range of the experimental excitation wavelengths (Fig.S19-S21). The intensities of the LnW_{10} luminescence decrease with the redshift of the excitation wavelengths, while the emission intensities of quinine increase. As a result, accompanied with the shift of the excitation wavelengths, tunable emission colors covering the full visible region were realized within several mixture solutions, and the white color with CIE values (0.34, 0.33) was achieved in TbW_{10}/EuW_{10}/quinine = 50/1/3 excited at 285nm

(Fig.3 and Table 2). The coincidence of the measurement and estimation indicates that another kind of "molecular pixels" can be accomplished in fixed components by varying the excitation wavelengths.

Thus, comprehensively and firmly, the results of emission spectra, fluorescent lifetimes, and chromaticity coordinates of all the mixtures above demonstrated block of energy transfer crosstalk in aqueous solutions. We proposed that encapsulation of LnW_{10} by the cationic blocks of the copolymer would spatially isolate LnW_{10} species and obstruct the energy transfer between lanthanides. In addition, well dispersion of quinine in water, instead of participating into the assemblies, chiefly eliminated energy transfer between quinine and lanthanides. If the quinine group was conjugated into the copolymers to co-assemble with LnW_{10} into the aggregates, its emission spectra unexpectedly changed with mixing ratios, indicative of occurrence of energy transfer (from unpublished results).

Various desired luminescence color can be precisely predicted in solution through superposition of the emission spectra of the primary-color molecules at proper ratios and corresponding excitation wavelengths, avoiding the time-consuming and laborious repetitions of mixing and testing process.

Table 1 Summary of lifetimes τ_1 and τ_2 and corresponding fractions α_1 and α_2, and CIE coordinates (estimated and experimental) of hybrid binary and ternary mixtures at different molar ratios excited under 280 nm.

	ratio	τ_1 (ms)	α_1 (%)	τ_2 (ms)	α_2 (%)	CIE (estimated)	CIE (measured)
TbW_{10}/ EuW_{10}	10/1	1.280	7.56	4.386	92.44	(0.56, 0.41)	(0.56, 0.41)
	25/1	1.195	8.51	4.323	91.49	(0.50, 0.44)	(0.49, 0.44)
	50/1	1.510	17.16	4.389	82.84	(0.45, 0.47)	(0.45, 0.47)
	75/1	1.468	17.95	4.229	82.05	(0.42, 0.49)	(0.41, 0.49)
	150/1	1.408	25.62	3.975	74.38	(0.38, 0.52)	(0.37, 0.51)
TbW_{10}/ Quinine	2/1	1.049	15.95	2.590	84.05	(0.19, 0.17)	(0.19, 0.17)
	5/1	0.839	14.26	2.254	85.74	(0.23, 0.28)	(0.23, 0.26)
	10/1	0.944	17.40	2.364	82.60	(0.25, 0.36)	(0.25, 0.35)
	20/1	0.928	16.34	2.520	83.66	(0.27, 0.43)	(0.27, 0.42)
	50/1	0.996	17.19	2.480	82.81	(0.29, 0.49)	(0.29, 0.48)
EuW_{10}/ Quinine	5/1	1.720	4.39	4.380	95.61	(0.60, 0.36)	(0.60, 0.36)
	2/1	0.963	2.14	4.373	97.86	(0.57, 0.34)	(0.57, 0.35)
	1/1	1.065	2.78	4.406	97.22	(0.53, 0.31)	(0.53, 0.32)
White1		1.458	15.60	4.256	84.38	(0.33, 0.33)	(0.34, 0.33)

Table 2 Estimated and experimental CIE coordinates of TbW_{10}/EuW_{10} = 30/1, EuW_{10}/Quinine = 3/1, and TbW_{10}/EuW_{10}/Quinine = 50/1/3 hybrid mixtures under different excitation wavelengths.

	λ_{ex} (nm)	CIE (estimated)	CIE (measured)
TbW_{10}/ Quinine	280	(0.27, 0.43)	(0.27, 0.43)
	290	(0.25, 0.35)	(0.25, 0.36)
	300	(0.22, 0.28)	(0.23, 0.28)
	310	(0.18, 0.16)	(0.18, 0.16)
EuW_{10}/ Quinine	280	(0.56, 0.34)	(0.56, 0.35)
	290	(0.52, 0.31)	(0.52, 0.32)
	300	(0.45, 0.27)	(0.45, 0.27)
	305	(0.37, 0.22)	(0.37, 0.22)
	310	(0.26, 0.16)	(0.27, 0.16)
TbW_{10}/ EuW_{10}/ Quinine	270	(0.38, 0.39)	(0.39, 0.40)
	280	(0.36, 0.37)	(0.36, 0.37)
	285	(0.33, 0.33)	(0.34, 0.33)
	290	(0.30, 0.30)	(0.30, 0.30)
	295	(0.28, 0.26)	(0.28, 0.27)
	300	(0.25, 0.23)	(0.25, 0.23)
	305	(0.22, 0.17)	(0.22, 0.17)

Luminescent properties of hybrid films

The compatibility of inorganic molecules, organic small molecules, as well as processable polymers, offers a chance for the mixtures to be conveniently used as materials. Homogeneous, transparent, and self-supporting films were fabricated after extracting the mixture solution by PMMA and then casting on quartz (Fig.S23). Although LnW_{10} is immiscible with organic solvents or PMMA matrix, formation of LnW_{10}/BCP micelles improves the compatibility between LnW_{10} and PMMA, and makes it easy to integrate the three luminophores uniformly dispersed in the PMMA matrix to produce the homogeneous films.

Unlike most organic systems, neither hypsochromic nor bathochromic shift of luminescence took place manifestly in the visible region in these films, with the CIE coordinates (0.29, 0.46) for G, (0.60, 0.38) for R, and (0.18, 0.10) for B. Only single lifetime, 1.550 ms, was fitted for G, and R exhibited a long lifetime of 3.553 ms (95.30%) and a short lifetime of 0.808 ms (4.70%). The lifetimes of films were faintly altered from solution samples, owing to the slightly different microenvironment of the luminophores. Absolute luminescent quantum yields $\Phi_{ab, FL}$ were measured as 0.161 for R, 0.001 for B and <0.001 for G. The disparity of the isostructural LnW_{10} quantum

yields arises from the nonradioactive Tb^{4+} - W^{5+} energy transfer in TbW_{10}, greatly decreasing the quantum yield of TbW_{10}[56].

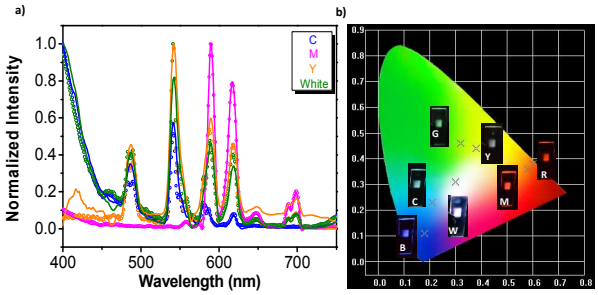

Fig. 4 a) Emission spectra of representative thin films. Solid lines are measured results and unfilled circles represent estimated spectra. b) Emission coordinates of films in the CIE 1931 chromaticity diagram. Insets are photographs of corresponding samples on quartz excited under 280 nm.

Table 3 Summary of lifetimes τ_1 and τ_2 and corresponding fractions α_1 and α_2, and CIE coordinates (estimated and experimental) of M, Y, C, and White thin films excited under 280 nm.

	M	Y	C	White
τ_1 (ms)	1.653	0.923	1.565	0.335
α_1 (%)	16.77	17.45	100.00	5.21
τ_2 (ms)	3.777	2.734	-	2.606
α_2 (%)	83.23	82.55	-	94.79
CIE (estimation)	(0.57, 0.36)	(0.38, 0.43)	(0.21, 0.23)	(0.30, 0.31)
CIE (experiment)	(0.58, 0.36)	(0.38, 0.43)	(0.21, 0.23)	(0.30, 0.31)

The molecular pixels performance of the solutions was preserved in solid films. A white color as well as secondary colors such as yellow (Y), magenta (M), and cyan (C) within the triangle were selected to assess the molecular pixels system by reproducing colors in the xy chromaticity diagram. Emission spectra (measured and estimated), CIE coordinates (measured and estimated), and luminescence lifetimes of the films were shown in Fig.4 and Table 3. The film of TbW_{10}/EuW_{10}/quinine = 100/1/20 was expected to produce a white color with chromaticity coordinates of (0.30, 0.31), which is well consistent with the experimental CIE coordinates, (0.30, 0.31), excited at 280 nm. Besides, the luminescence lifetimes of each film supported that their molecular pixels properties benefit from the suppressed energy transfer. But limited by the dominant

amount of the low quantum yield of TbW_{10}, the quantum yield of white emission film was lower than 0.001. Improving the luminescent efficiencies is one of the objectives in our future research.

Conclusions

We successfully constructed multicolor luminescent hybrid supramolecular assembled materials consisting of isostructural red and green luminescent inorganic clusters incorporated into the core-shell micelles through electrostatic interaction with neutral-cationic double hydrophilic block copolymers, as well as blue luminescent quinine well-dispersed outside the micelles. Luminophores are effectively isolated with each other by the block copolymers in aqueous solution, and polymer matrix, which suppressed the undesired intermolecular energy transfer crosstalk between inorganic and organic luminophores. The emission spectra are independent under various mixing ratios and excitation wavelengths. The three primary color-emitting luminophores behave as molecular pixels in both solutions and films that desired emission colors within the gamut can be realized through precise prediction on the basis of additive color theory. This general and straightforward approach essentially avoids the repetitive trials, and paves a way for potential applications in displays and luminescent sensors.

Acknowledgements

We would like to thank Prof. Jun Lin and Dr. Yang Zhang at Changchun Institute of Applied Chemistry, Chinese Academy of Sciences for their kind help on PLQY measurement. This work was supported by the National Natural Science Foundation of China (No. 21322404; No. 51373001), and the Beijing Natural Science Foundation (No. 2122024).

References

1. P. Andersson, D. Nilsson, P. O. Svensson, M. Chen, A. Malmström, T. Remonen, T. Kugler and M. Berggren, *Advanced Materials*, 2002, **14**, 1460-1464.
2. R. Tian, R. Liang, D. Yan, W. Shi, X. Yu, M. Wei, L. S. Li, D. G. Evans and X. Duan, *J. Mater. Chem. C*, 2013, **1**, 5654-5660.
3. C. D. Müller, A. Falcou, N. Reckefuss, M. Rojahn, V. Wiederhirn, P. Rudati, H. Frohne, O. Nuyken, H. Becker, K. Meerholz, *Nature*, 2003, **421**, 829.
4. L. Xiao, Z. Chen, B. Qu, J. Luo, S. Kong, Q. Gong and J. Kido, *Adv. Mater.*, 2011, **23**, 926-952.
5. S. V. Eliseeva and J. C. G. Bunzli, *Chem. Soc. Rev.*, 2010, **39**, 189-227.
6. Z. Chen, X. Wu, S. Hu, P. Hu, H. Yan, Z. Tang and Y. Liu, *J. Mater. Chem. C*, 2015, **3**, 153-161.
7. Y. Chen, L. Qiao, L. Ji and H. Chao, *Biomaterials*, 2014, **35**, 2-13.
8. J. Yu, X. Diao, X. Zhang, X. Chen, X. Hao, W. Li, X. Zhang and C. S. Lee, *Small*, 2014, **10**, 1125-1132.

9. H. C. Peng, C. C. Kang, M. R. Liang, C. Y. Chen, A. Demchenko, C. T. Chen and P. T. Chou, *ACS Appl. Mater. Interfaces*, 2011, **3**, 1713-1720.
10. Y. Wada, M. Sato and Y. Tsukahara, *Angew. Chem. Inter. Ed.*, 2006, **45**, 1925-1928.
11. C. Vijayakumar, V. K. Praveen and A. Ajayaghosh, *Adv. Mater.*, 2009, **21**, 2059-2063.
12. H. Kim and J. Young Chang, *RSC Adv.*, 2013, **3**, 1774-1780.
13. Y. Yang, M. Lowry, C. M. Schowalter, S. O. Fakayode, J. O. Escobedo, X. Xu, H. Zhang, T. J. Jensen, F. R. Fronczek, I. M. Warner and R. M. Strongin, *J. Am. Chem. Soc.*, 2006, **128**, 14081-14092.
14. C. Yuan, S. Saito, C. Camacho, S. Irle, I. Hisaki and S. Yamaguchi, *J. Am. Chem. Soc.*, 2013, **135**, 8842-8845.
15. C. Giansante, G. Raffy, C. Schäfer, H. Rahma, M. T. Kao, A. G. L. Olive and A. Del Guerzo, *J. Am. Chem. Soc.,* 2010, **133**, 316-325.
16. A. Yin, Y. Zhang, L. Sun and C. Yan, *Nanoscale*, 2010, **2**, 953-959.
17. B. Bao, N. Tao, D. Yang, L. Yuwen, L. Weng, Q. Fan, W. Huang and L. Wang, *Chem. Commun.*, 2013, **49**, 10623-10625.
18. J. Luo, X. Li, Q. Hou, J. B. Peng, W. Yang and Y. Cao, *Adv. Mater.*, 2007, **19**, 1113-1117.
19. Y. Shiraishi, C. Ichimura, S. Sumiya and T. Hirai, *Chem. Eur. J.*, 2011, 17, 8324-8332.
20. B. Yan and Y. F. Shao, *RSC Adv.*, 2014, **4**, 3318.
21. P. T. Furuta, L. Deng, S. Garon, M. E. Thompson and J. M. J. Fréchet, *J. Am. Chem. Soc.*, 2004, **126**, 15388-15389.
22. M. Mao, C. Zhou, H. Shen, H. Wang, S. Wang and L. S. Li, *Mater. Lett.*, 2013, **111**, 97-100.
23. J. Chen, F. Zeng, S. Wu, J. Su and Z. Tong, *Small*, 2009, **5**, 970-978.
24. H. F. Gao, D. A. Poulsen, B. W. Ma, D. A. Unruh, X. Y. Zhao, J. E. Millstone and J. M. J. Frechet, *Nano. Lett.*, 2010, **10**, 1440-1444.
25. J. Malinge, C. Allain, A. Brosseau and P. Audebert, *Angew. Chem. Inter. Ed.*, 2012, **51**, 8534-8537.
26. Q. Chen, D. Zhang, G. Zhang, X. Yang, Y. Feng, Q. Fan and D. Zhu, *Adv. Func. Mater.*, 2010, **20**, 3244-3251.
27. M. Higuchi, *J. Mater. Chem. C*, 2014, **2**, 9331-9341.
28. E. W. Meijer, *J. Am. Chem. Soc.*, 2009, **131**, 833-843.
29. S. Brovelli, G. Sforazzini, M. Serri, G. Winroth, K. Suzuki, F. Meinardi, H. L. Anderson and F. Cacialli, *Adv. Func. Mater.*, 2012, **22**, 4284-4291.
30. J. R. Lakowicz, *Principles of Fluorescence Spectroscopy*, 3rd ed.; Springer: New York, 2006.
31. H. Shono, T. Ohkawa, H. Tomoda, T. Mutai and K. Araki, *ACS Appl. Mater. Interfaces*, 2011, **3**, 654-657.
32. J. E. Kwon, S. Park and S. Y. Park, *J. Am. Chem. Soc.*, 2013, **135**, 11239-11246.
33. H. Gao, D. A. Poulsen, B. Ma, D. A. Unruh, X. Zhao, J. E. Millstone and J. M. J. Fréchet, *Nano. Lett.*, 2010, **10**, 1440-1444.
34. Y. Shiraishi, Y. Furubayashi, G. Nishimura and T. Hirai, *Journal of Luminescence*, 2007, **126**, 68-76.
35. Y. Wei, Q. Li, R. Sa and K. Wu, *Chem. Commun.*, 2014, **50**, 1820-1823.
36. T. R. Zhang, S. Q. Liu, Dirk G. Kurth and Charl F. J. Faul, *Adv. Funct. Mater.* 2009, **19**, 642-652.
37. Z. F. Liu, M. F. Wu, S. H. Wang, F. K. Zheng, G. E. Wang, J. Chen, Y. Xiao, A. Q. Wu, G. C. Guo and J. S. Huang, *J. Mater. Chem. C*, 2013, **1**, 4634-4639.
38. Y. S. Liu, D. T. Tu, H. M. Zhu and X. Y. Chen, *Chem. Soc. Rev.*, 2013, **42**, 6924-6958.
39. D. Tu, W. Zheng, Y. Liu, H. Zhu and X. Chen, *Coord. Chem. Rev.*, 2014, **273–274**, 13-29.
40. X. Wang, H. Chang, J. Xie, B. Zhao, B. Liu, S. Xu, W. Pei, N. Ren, L. Huang and W. Huang, *Coord. Chem. Rev.*, 2014, **273–274**, 201-212.
41. H. Zhang, X. Shan, L. Zhou, P. Lin, R. Li, E. Ma, X. Guo and S. Du, *J. Mater. Chem. C*, 2013, **1**, 888-891.
42. Y. Cui, H. Xu, Y. Yue, Z. Guo, J. Yu, Z. Chen, J. Gao, Y. Yang, G. Qian and B. Chen, *J. Am. Chem. Soc.*, 2012, **134**, 3979-3982.
43. P. R. Matthes, C. J. Holler, M. Mai, J. Heck, S. J. Sedlmaier, S. Schmiechen, C. Feldmann, W. Schnick and K. Muller-Buschbaum, *J. Mater. Chem.*, 2012, **22**, 10179-10187.
44. S. L. Zhong, R. Xu, L. F. Zhang, W. G. Qu, G. Q. Gao, X. L. Wu and A. W. Xu, *J. Mater. Chem.*, 2011, **21**, 16574-16580.

45. K. Binnemans, *Chem. Rev.*, 2009, **109**, 4283-4374.
46. G. He, D. Guo, C. He, X. Zhang, X. Zhao and C. Duan, *Angew. Chem. Int. Ed.*, 2009, **48**, 6132-6135.
47. J. Feng and H. J. Zhang, *Chem. Soc. Rev.*, 2013, **42**, 387-410.
48. R. D. Peacock and T. J. R. Weakley, *J. Chem. Soc. A*, 1971, 1836-1839.
49. H. B. Wei, S. M. Du, Y. Liu, H. X. Zhao, C. Y. Chen, Z. B. Li, J. Lin, Y. Zhang, J. Zhang and X. H. Wan, *Chem. Commun.,* 2014, **50**, 1447-1450.
50. Y. Liu, H. X. Zhao, H. B. Wei, N. Shi, J. Zhang and X. H. Wan, *J. Inorg. Organomet. Polym. Mater.*, 2015, **25**, 126-132.
51. H. B. Wei, N. Shi, J. L. Zhang, Y. Guan, J. Zhang and X. H. Wan, *Chem. Commun.*, 2014, **50**, 9333-9335.
52. R. Ballardini, Q. G. Mulazzani, M. Venturi, F. Bolletta and V. Balzani, *Inorg. Chem. Commun.*, 1984, **23**, 300-305.
53. W. D. Horrocks and D. R. Sudnick, *Acc. Chem. Res.*, 1981, **14**, 384-392.
54. W. D. Horrocks and D. R. Sudnick, *J. Am. Chem. Soc.*, 1979, **101**, 334-340.
55. J. Zhang, Y. Liu, Y. Li, H. Zhao and X. Wan, *Angew. Chem. Inter. Ed.*, 2012, **51**, 4598-4602.
56. A. B. Yusov, and A. M. Fedoseev, *J. Appl. Spectrosc.* 1988, **49**, 1248-1253.